

Pasha Apontes,¹ Zhongbo Liu,¹ Kai Su,² Outhiriaradjou Benard,¹ Dou Y. Youn,³ Xisong Li,¹ Wei Li,³ Raihan H. Mirza,¹ Claire C. Bastie,¹ Linda A. Jelicks,⁴ Jeffrey E. Pessin,^{1,5} Radhika H. Muzumdar,² Anthony A. Sauve,³ and Yuling Chi¹



Mangiferin Stimulates Carbohydrate Oxidation and Protects Against Metabolic Disorders Induced by High-Fat Diets

Diabetes 2014;63:3626–3636 | DOI: 10.2337/db14-0006

Excessive dietary fat intake causes systemic metabolic toxicity, manifested in weight gain, hyperglycemia, and insulin resistance. In addition, carbohydrate utilization as a fuel is substantially inhibited. Correction or reversal of these effects during high-fat diet (HFD) intake is of exceptional interest in light of widespread occurrence of diet-associated metabolic disorders in global human populations. Here we report that mangiferin (MGF), a natural compound (the predominant constituent of *Mangifera indica* extract from the plant that produces mango), protected against HFD-induced weight gain, increased aerobic mitochondrial capacity and thermogenesis, and improved glucose and insulin profiles. To obtain mechanistic insight into the basis for these effects, we determined that mice exposed to an HFD combined with MGF exhibited a substantial shift in respiratory quotient from fatty acid toward carbohydrate utilization. MGF treatment significantly increased glucose oxidation in muscle of HFD-fed mice without changing fatty acid oxidation. These results indicate that MGF redirects fuel utilization toward carbohydrates. In cultured C2C12 myotubes, MGF increased glucose and pyruvate oxidation and ATP production without affecting fatty acid oxidation, confirming in vivo and ex vivo effects. Furthermore, MGF inhibited anaerobic metabolism of pyruvate to lactate but enhanced pyruvate oxidation. A key target

of MGF appears to be pyruvate dehydrogenase, determined to be activated by MGF in a variety of assays. These findings underscore the therapeutic potential of activation of carbohydrate utilization in correction of metabolic syndrome and highlight the potential of MGF to serve as a model compound that can elicit fuel-switching effects.

The worldwide incidence of diabetes was estimated to be 347 million in 2008 and has been projected to continue to increase (1). The most important driving force for this high incidence of diabetes is an increasing prevalence of obesity (2) linked to consumption of high-calorie foods and sedentary activity. Although lifestyle changes can mitigate some of the prevailing metabolic syndrome in obese populations, targeted therapies that modify fundamental cellular and physiologic processes are needed for long-term medical success in treating this epidemic. Cellular dysfunction includes mitochondrial deterioration, which has been implicated as a fundamental feature accompanying type 2 diabetes. Previous studies have demonstrated that pharmacologic or genetic upregulation of mitochondrial functions can provide favorable outcomes in diet-induced metabolic syndromes (3,4).

¹Department of Medicine, Albert Einstein College of Medicine, Bronx, NY

²Department of Paediatrics, Albert Einstein College of Medicine, Bronx, NY

³Department of Pharmacology, Weill Cornell Medical College, New York, NY

⁴Department of Physiology & Biophysics and Gruss Magnetic Resonance Research Center, Albert Einstein College of Medicine, Bronx, NY

⁵Department of Molecular Pharmacology, Albert Einstein College of Medicine, Bronx, NY

Corresponding author: Yuling Chi, yuling.chi@einstein.yu.edu.

Received 3 January 2014 and accepted 16 May 2014.

This article contains Supplementary Data online at <http://diabetes.diabetesjournals.org/lookup/suppl/doi:10.2337/db14-0006/-/DC1>.

© 2014 by the American Diabetes Association. Readers may use this article as long as the work is properly cited, the use is educational and not for profit, and the work is not altered.

Although enhancing fatty acid oxidation can reduce fat accumulation, it may not directly mitigate hyperglycemia, because fatty acid oxidation inhibits glucose utilization (5,6). Dietary overconsumption of fats/lipids enhances fatty acid fuel utilization but induces metabolic inflexibility and insulin resistance (7), even when accompanied by increased mitochondrial density and increased oxidative capacities (8,9). This conundrum at least theoretically weakens strategies for increasing fatty acid oxidation as a means to rescue animals subject to metabolic disorders induced by a high-fat diet (HFD). We argue that an alternative and key consideration associated with strategies that seek enhanced oxidative metabolism is whether they can promote glucose utilization, which could improve glucose profiles and mitigate insulin resistance.

Skeletal muscle is the major peripheral tissue that removes blood glucose, accounting for ~75% of whole-body glucose uptake (6). After uptake into tissues, glucose is metabolized into different pathways, with a major catabolite being pyruvate, a central branch-point metabolite in carbohydrate metabolism. Subject to regulatory factors, pyruvate is converted to several downstream metabolites, including alanine, oxaloacetate, lactate, and acetyl-CoA, with the last two as major metabolites (10). The irreversible conversion of pyruvate to acetyl-CoA, catalyzed by pyruvate dehydrogenase (PDH), provides a regulatory step by which glucose enters into oxidative metabolism. Alternatively, conversion of pyruvate to lactate by lactate dehydrogenase (LDH) (10) enables muscle release of lactate for the Cori cycle from muscle to liver.

PDH serves as a central gatekeeper of carbohydrate oxidative metabolism. PDH activity regulates the fate of carbohydrate metabolism in muscle as the determining factor in setting the competition between glucose and fatty acid catabolism in this tissue (7,11). Decreased PDH activity is proposed to be a fundamental factor in the derangement of carbohydrate metabolism (12) observed in diabetic heart and skeletal muscle (13,14). Activation of PDH by dichloroacetate (DCA) or by deletion of the negative regulator, PDH kinase (PDK), improves muscle functions, lowers glucose levels, and increases glucose tolerance and insulin sensitivity in mice and humans (15,16). These data indicate that improved carbohydrate utilization linked to activation of key metabolic steps can provide fundamental improvements in metabolic syndrome.

In this study, we report that stimulation of carbohydrate oxidation is the pharmacodynamic outcome of a natural product, mangiferin (MGF), the predominant constituent of *Mangifera indica* bark extract (mango tree; Supplementary Fig. 1). Mice treated with MGF were protected from HFD-induced toxicities, including weight gain, insulin resistance, and glucose intolerance. Further investigation into its mechanisms of actions demonstrated that MGF activates PDH, thereby increasing carbohydrate oxidation and metabolic flexibility of energy substrate utilization.

RESEARCH DESIGN AND METHODS

Chemical reagents were purchased from Sigma-Aldrich (St. Louis, MO), unless specified. Animals were fed a chow diet (CD; Purina LabDiet, Framingham, MA) providing 28.5% (kcal) protein, 13.5% fat, and 58% carbohydrates, or an HFD (Research Diets, New Brunswick, NJ) providing 20% (kcal) protein, 60% fat, and 20% carbohydrates.

Animal Experiments

Wild-type C57BL6/J mice at the age of 5–6 weeks were purchased from The Jackson Laboratory (Bar Harbor, ME). All studies were approved by and performed in compliance with the guidelines of the Yeshiva University Institutional Animal Care and Use Committee. The CD and HFD were ground into fine powder and mixed with pure MGF (CTMedChem, Bronx, NY). The mixtures were repelleted and administered to individually housed mice. Mice were fed ad libitum with the CD or HFD, with or without MGF, and water.

Fat composition and fat distribution were determined by MRI. Lean and fat mass was determined as described (17). Metabolic measurements (V_{O_2}), respiratory quotient (RQ), energy expenditure (EE), and locomotor activity were obtained continuously using a CLAMS (Columbus Instruments) open-circuit indirect calorimetry system (18). Animals were acclimatized for 2 days, and data were subsequently collected over a 5-day period. Body temperature was measured using a BAT-10 thermometer (Physitemp, Clifton, NJ). Hyperinsulinemic-euglycemic clamps were performed as described (19). An intraperitoneal glucose tolerance test (IGTT) was performed on conscious mice after 12-h fasting and an intraperitoneal injection with 20% glucose in saline (2 g/kg total body weight).

Fatty Acid and Glucose Oxidation in Isolated Muscle

Palmitate and glucose oxidation in soleus muscle were measured using previously described methods (20,21), with slight modification. Soleus muscle was incubated in the oxidation buffer for 1 h for palmitate oxidation and for 6 h for glucose oxidation.

Cell Culture

C2C12 myoblast cells were maintained in DMEM high glucose (HyClone Laboratories, Logan, UT), supplemented with 1% penicillin and streptomycin (Gibco, Carlsbad, CA) and 10% FBS. C2C12 cells were differentiated in the above DMEM medium containing 2% horse serum (replacing 10% FBS) for 4–6 days after cells reached confluence.

Fatty acid oxidation in myotubes was measured by radioactivity assay using methods as described (22).

Oxygen Consumption Rate and Extracellular Acidification Rate Measurements by Metabolic Flux Analyzer

Oxygen consumption rate (OCR) and extracellular acidification rate (ECAR) in C2C12 myotubes were obtained by a Metabolic Flux analyzer (Seahorse Bioscience), as previously described (23,24). In brief, myotubes differentiated

from C2C12 cells in XF24 microplates were incubated overnight in glucose-free and sodium pyruvate-free DMEM containing L-glutamine, 2% horse serum, and 1% penicillin/streptomycin, with or without 200 $\mu\text{mol/L}$ MGF. The concentrations of MGF used for this and the subsequent in vitro assays were chosen based on the in vivo effective dose of 400 mg/kg body weight and oral MGF bioavailability of 1.2% in rat (25). Medium containing vehicle, BSA-conjugated palmitate, D-glucose, or sodium pyruvate was loaded in port A of the sensor cartridge, and 70 μL was injected to wells containing 630 μL media. The final concentrations of BSA-palmitate, D-glucose, and sodium pyruvate were 0.1, 25, and 50 mmol/L, respectively.

Mitochondrial Protein Preparation

Mitochondria were isolated from C2C12 myotubes treated with various concentrations of MGF for 24 h or with various concentrations of MGF, 5 mmol/L DCA, or 2 mmol/L fluoropyruvate (FP) plus 0.2 mmol/L MGF for 15 min, at 37°C, using the previously described method (26,27) with modified buffer (250 mmol/L sucrose, 1 mmol/L EGTA, 10 mmol/L HEPES, and 5 g/L BSA, pH 7.5). Mitochondrion pellets were suspended, and mitochondrial protein was extracted by a freeze-thaw procedure (26,27).

PDH Activity

Spectrometry Assay

As adapted from previous reports (26,28,29), 100 μg mitochondrial protein lysate was loaded in a 96-well plate in 200 μL reaction buffer containing 5 mmol/L L-carnitine, 2.5 mmol/L NAD⁺, 0.2 mmol/L thiamine pyrophosphate, 0.1 mmol/L CoA, 1 mL/L Triton X-100, 0.3 mmol/L DTT, 1 mmol/L MgCl₂, 1 g/L BSA, and 6.5 mol/L phenazine methosulfate in 50 mmol/L potassium phosphate buffer (pH 7.5). Reaction was initiated by adding 5 mmol/L pyruvate (50 μL) and 0.6 mmol/L p-iodonitrotetrazolium violet.

Radioactivity Assay

We developed a system based on previous reports (27,30–32), in which a manifold was used to split the airflow into six branches that were simultaneously connected to six pairs of reaction and trapping vials. Into each reaction vial was added 200 μL reaction buffer (1 mmol/L MgCl₂, 1 mmol/L DTT, 0.1 mmol/L thiamine pyrophosphate, 0.3 mmol/L CoA, 2.5 mmol/L NAD⁺, 50 mmol/L potassium phosphate, 75 $\mu\text{mol/L}$ sodium pyruvate, freshly prepared, pH 8.0), and 0.2 μL [carboxy-¹⁴C]-labeled pyruvate (0.1 $\mu\text{Ci}/\mu\text{L}$, 55 $\mu\text{Ci}/\mu\text{mol}$). Into each trapping vial was added 300 μL trapping solution (1 mmol/L NaOH). After airflow was stabilized, mitochondrial protein lysate (10–50 μg) was injected into the reaction vial. At various time points (3–40 min), reactions were stopped by injecting 10% trichloroacetic acid (250 μL), and ¹⁴CO₂ was trapped for 3 h. Reaction and trapping were performed at room temperature. ¹⁴C in trapping and reaction vials was counted separately by a scintillation counter. Statistical analyses are specified in the figure legends.

RESULTS

MGF Protects Against HFD-Induced Obesity

A report indicated that MGF treatment in a type 2 diabetic mouse model (KK-Ay mice) improved the glucose and insulin profile (33). To evaluate MGF effects on HFD-induced insulin resistance and obesity, C57BL/6J mice were fed the CD or HFD containing 0%, 2.5%, or 5.0% g MGF/g food. Mice fed the CD supplemented with MGF exhibited similar weight gain as controls (Fig. 1A). When challenged with the HFD, mice experienced substantial weight gain compared with CD mice over a 16-week period. MGF treatments decreased HFD-induced weight gain in a dose-dependent manner (Fig. 1A). After 5 weeks, 0.5% MGF (~400 mg/kg as a result of average daily food intake of 2–3 g) produced statistically significant weight reduction. Impressively, continued treatment with MGF

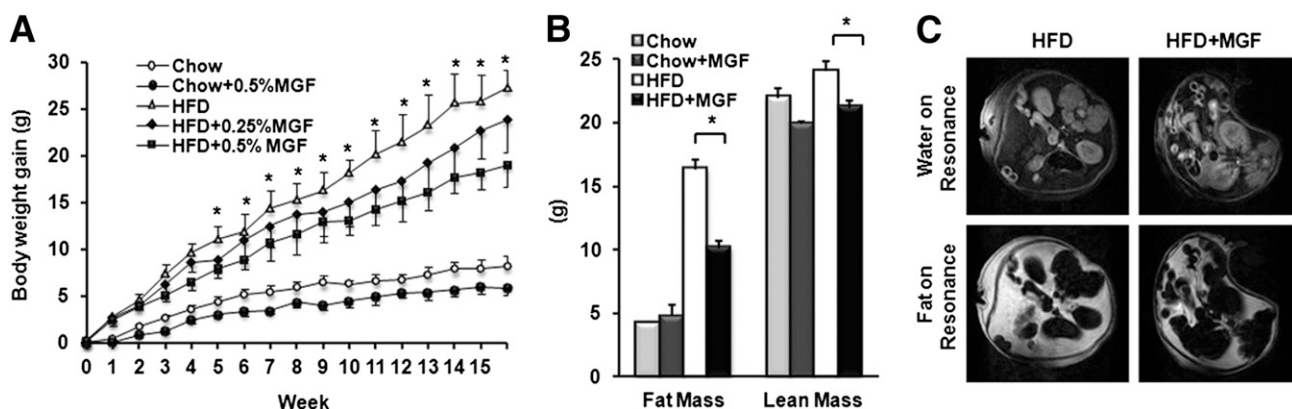


Figure 1—MGF mitigates HFD-induced obesity. C57BL/6J mice (5–6 weeks old) were fed with CD or HFD, with or without MGF (0, 0.25%, 0.5% g/g), for 16 weeks ($n = 10$ per group). Body weight was monitored daily. **A**: Graph of body weight gain over time. * $P < 0.05$ indicates significant changes between HFD and HFD + 0.5% MGF groups. **B**: Body composition evaluated by nuclear magnetic resonance after 16 weeks of diet. * $P < 0.05$. Values are average \pm SEM. **C**: MRI of two representative mice fed with HFD or HFD + 0.5% MGF for 16 weeks. “Water on resonance” is the typical MRI image at the level of the kidneys. “Fat on resonance” shows the same anatomic location with the transmitter set on the fat resonance to show fat distribution. P values were obtained by ANOVA test.

for 16 weeks prevented 50% of the body weight gain of the HFD-fed mice (Fig. 1A). Nuclear magnetic resonance-based whole-body fat quantitation revealed that MGF decreased total fat mass (Fig. 1B), accounting for most of the weight difference observed between treated and untreated animals. MGF also modestly reduced lean mass (Fig. 1B) because lean mass loss often accompanies fat mass loss (34). MRI cross-sectional images showed that abdominal fat accumulation was largely prevented by MGF treatment (Fig. 1C).

MGF Enhances Systemic Respiration and EE

To further investigate the physiologic basis for the reduced body weight gain in MGF-treated animals, we quantified

caloric intake and EE by indirect calorimetry (Fig. 2). MGF did not affect food or water intake (Fig. 2A). In CD-fed mice, MGF treatment caused a slight increase in activity in the dark cycle (Fig. 2B) but no change in total spontaneous locomotor activity (Fig. 2C). In HFD-fed mice, MGF modestly increased locomotor activity in nocturnal hours. EE was increased in mice fed the MGF-treated HFD (Fig. 2D and E), which was correlated with increased VO_2 (Supplementary Fig. 2). The increase in spontaneous locomotor activity was marginal and consistent with spontaneous locomotor activity being insufficient to account for alterations in EE in standard mouse caging (35), suggesting that MGF-caused increases in EE were from activity-independent metabolic processes.

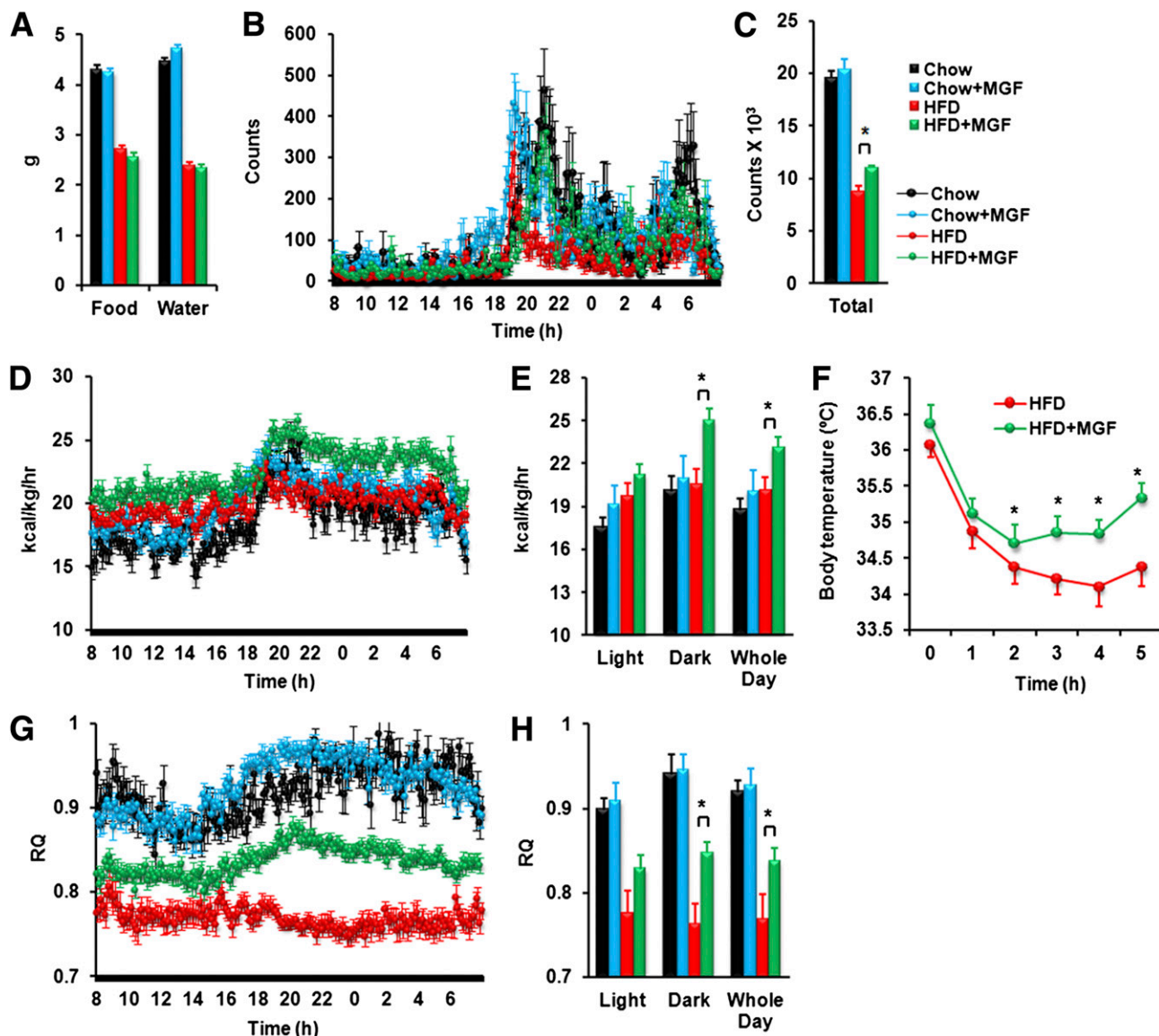


Figure 2—MGF enhances EE and promotes carbohydrate utilization in vivo. C57BL6/J mice (5–6 weeks old) were fed with CD or HFD or those diets mixed a dose of 0.5% MGF for 16 weeks ($n = 10$ per group). A: Average daily food and water intake. Indirect calorimetry assessments of locomotor activity (B and C), EE (D and E), and RQ (G and H). F: Cold test. Body temperature was monitored while mice were exposed to 4°C for 5 h. * $P < 0.05$. P values were obtained by t test for F and by ANOVA test for the rest. Values are average \pm SEM.

An additional pathway for dissipation of energy is thermogenesis. MGF modestly increased basal body temperature when mice were maintained at an ambient temperature (Fig. 2*F*). This effect was more pronounced when mice were exposed to cold, highlighting an increased thermogenic capacity in MGF-treated animals, probably resulting from MGF-induced uncoupling proteins in brown adipose tissue (Supplementary Fig. 3).

MGF Stimulates Carbohydrate Utilization and Increases Flexibility in Use of Energy Substrates

We measured RQ to investigate whether MGF exerted changes in energy metabolism and metabolic fuel source selection. In untreated CD mice, RQ was ~ 0.9 during light hours and gradually increased during dark hours to 0.93, and MGF had a minimal effect (Fig. 2*G* and *H*). In untreated HFD-fed mice, RQ averaged at 0.77 at all times, demonstrating a striking shift to fatty acids as preferred fuels and apparent metabolic inflexibility (Fig. 2*G* and *H*). MGF treatment in HFD-fed mice increased RQ and RQ fluctuation, causing a range of 0.81–0.85 during the light and dark cycles (Fig. 2*G* and *H*). These data indicate that MGF promotes carbohydrate oxidation and improves fuel source flexibility.

MGF Protects Against HFD-Induced Glucose Intolerance and Insulin Resistance

Fasting plasma glucose was increased to 198 ± 25 mg/dL in 18-week HFD-fed mice compared with 116 ± 16 mg/dL in CD-fed controls (Fig. 3*A*). MGF treatment had no significant effect on glucose levels in CD mice but reduced the fasting glucose levels of HFD mice to 132 ± 7 mg/dL. HFD feeding drastically increased plasma insulin level to 2.93 ± 0.48 ng/mL from $\sim 0.75 \pm 0.12$ ng/mL in CD mice. MGF treatment resulted in a complete normalization of insulin levels in the HFD mice (Fig. 3*B*). To directly assess insulin sensitivity, we performed hyperinsulinemic-euglycemic clamp studies. As expected, HFD animals were insulin resistant compared with controls, as evidenced by a lower glucose infusion rate (GIR; Fig. 3*C*). MGF tripled the GIR in HFD animals, indicating that MGF improves insulin sensitivity.

One of the key factors affecting the GIR is the rate of glucose disposal by peripheral tissues such as muscle. MGF tripled the glucose disposal rate in HFD mice (Fig. 3*D*), providing direct evidence that MGF stimulates glucose utilization in muscle during HFD feeding. In an IGTT, MGF-treated HFD mice exhibited significantly improved glucose tolerance versus HFD mice, which were markedly glucose intolerant compared with CD mice (Fig. 3*E*). MGF-treated animals exhibited lower insulin levels at basal conditions and during the IGTT (Fig. 3*F*), consistent with MGF improvement of insulin sensitivity. MGF also modestly but significantly increased total plasma adiponectin in HFD mice (Fig. 3*G*) and prevented HFD-induced increase in plasma triglycerides (Fig. 3*H*), without any significant effect on free fatty acids (Fig. 3*I*).

MGF Promotes Carbohydrate Utilization

Improved glycemia and insulin sensitivity led us to connect the mechanism of action of MGF promotion of carbohydrate oxidation as indicated by the RQ. Glucose uptake data from the hyperinsulinemic-euglycemic clamp (Fig. 3*D*) also indicated enhanced glucose disposal and increased glucose catabolism. To further investigate these effects, we measured palmitate and glucose oxidation in the soleus skeletal muscle. HFD feeding doubled palmitate oxidation and conversely reduced glucose oxidation, consistent with prior reports (20,36). Interestingly, MGF did not significantly affect palmitate oxidation (Fig. 4*A*) but significantly increased glucose oxidation by 60% in HFD mice (Fig. 4*B*), suggesting that MGF preferentially enhances glucose utilization in the muscle.

To further evaluate MGF effects on fuel preference, fatty acid and glucose oxidation were both measured in cultured C2C12-derived myotubes. MGF did not significantly affect [carbonyl- ^{14}C]oleic acid oxidation in myotubes as measured by a radioactivity assay (Fig. 4*C*) nor did it affect palmitate OCR, as measured by the Seahorse Bioscience Metabolic Flux analyzer (Fig. 4*D*), consistent with the ex vivo results (Fig. 4*A*). We then monitored glucose catabolism in C2C12 myotubes by the Metabolic Flux analyzer. When treated with MGF, the myotube glucose oxidation rate was increased by $\sim 50\%$ (Fig. 4*E*). In addition, MGF accelerated glucose utilization as measured by time to peak (Fig. 4*E*). Some of this effect may be linked to MGF increased GLUT4 mRNA in the soleus muscle of HFD-fed mice and in C2C12 cells (Supplementary Fig. 4). These observations are consistent with ex vivo and in vivo results, confirming that MGF increases glucose metabolism, independent of fatty acid oxidation, even under a high dietary fat challenge. The MGF-stimulated increase in glucose metabolism also resulted in a statistically significant and dose-dependent increase in ATP production (Fig. 4*F*).

MGF Inhibits Lactic Acidosis

The end metabolite of glycolysis is pyruvate, which is a key intersection metabolite that can be converted by LDH to lactate or catabolized by PDH to acetyl-CoA. We first investigated whether MGF affected lactate formation. Using the Seahorse Bioscience analyzer, lactate production was monitored by the extracellular acidification of the media, ECAR of the media (23,24). Myotubes treated with glucose exhibited marked acidification of media, as measured by ECAR. Interestingly, MGF significantly blunted this effect (Fig. 5*A*).

Because ECAR is an indirect measure of lactate production, we directly measured lactate in the media in the Seahorse Bioscience plate. Indeed, media lactate in glucose-treated myotubes accumulated to ~ 80 nmol/L, and MGF reduced lactate accumulation to 30 nmol/L (Fig. 5*B*). In separate experiments, we determined that MGF inhibited lactate accumulation when glucose was fed to cells in a dose-dependent manner, with a half-maximal inhibitory concentration of 337 ± 40 $\mu\text{mol/L}$ (Fig. 5*C*), demonstrating

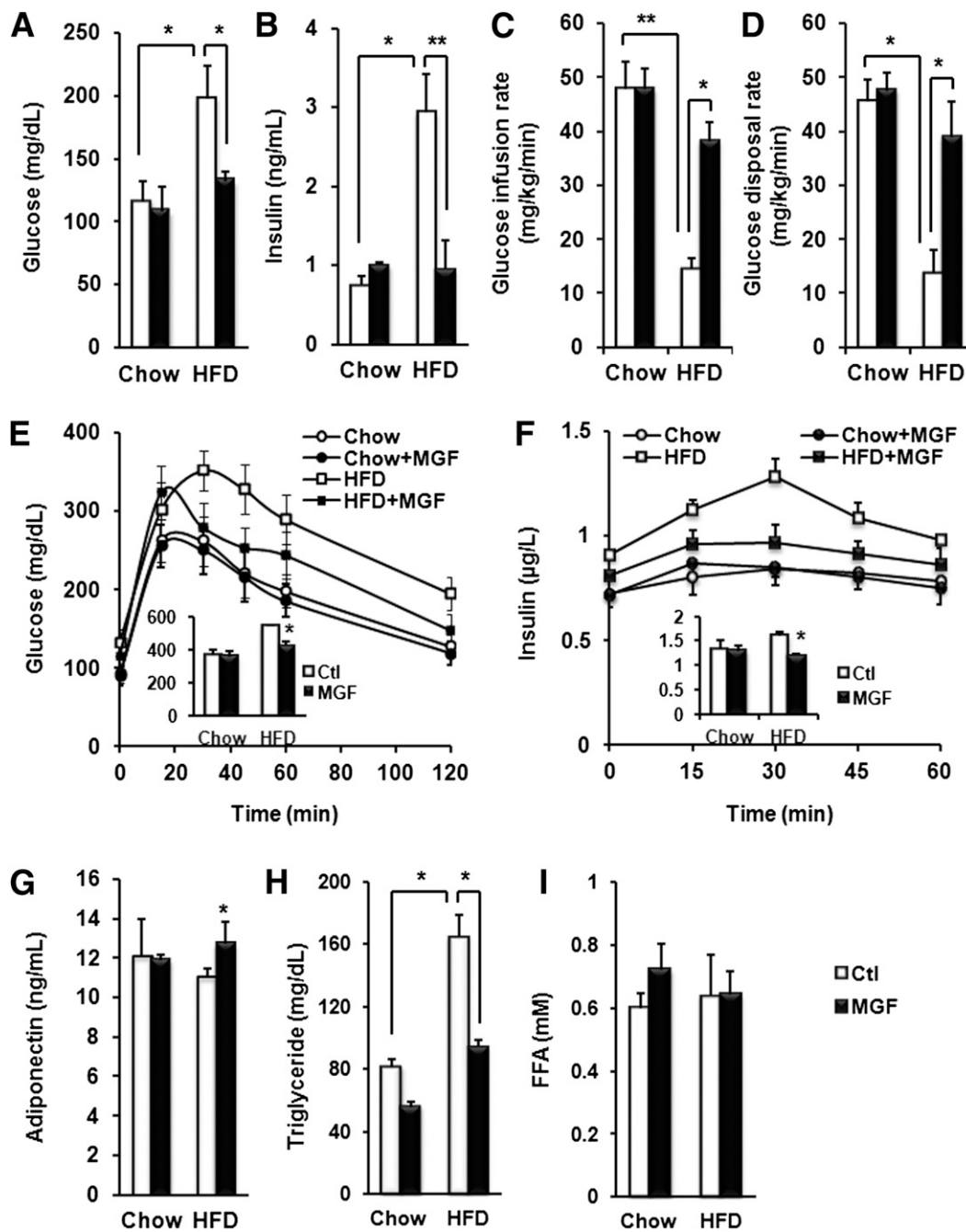


Figure 3—MGF protects against HFD-induced glucose intolerance and insulin resistance. Blood glucose (A), insulin (B), adiponectin (G), triglyceride (H), and free fatty acid (FFA) (I) levels were measured after a 12-h fast in animals fed with CD or HFD, with or without 0.5% MGF, for 16–18 weeks. GIR (C) and disposal rate (D) determined by hyperinsulinemic-euglycemic clamp assay performed on mice fed with CD or HFD, with or without 0.5% MGF, for 16–18 weeks. E: IGTT was performed after a 12-h fast on mice fed with CD or HFD, with or without 0.5% MGF, for 14 weeks. F: Insulin secretion during IGTT. Values are average ± SEM (n = 6–10 per group). *P < 0.05, **P < 0.01. P values were obtained by ANOVA test.

that MGF indeed inhibits lactate formation from glucose. Reduced lactate formation could be caused by direct inhibition of LDH or reduced availability of pyruvate to the fermentation pathway. We measured LDH activity using a kinetic assay with and without MGF and noted no effect on LDH activity (data not shown), suggesting that MGF might affect lactate production by enhancing pyruvate oxidation through PDH.

MGF Enhances Pyruvate Oxidation by Activating PDH

To determine if MGF activates PDH, C2C12 myotubes were incubated with pyruvate and displayed increased OCR. The addition of MGF with pyruvate resulted in both a larger OCR and temporal rate of activation (Fig. 6A), verifying that MGF enhances and accelerates oxidation of pyruvate (Fig. 6A) and glucose (Fig. 4E) as fuel substrates,

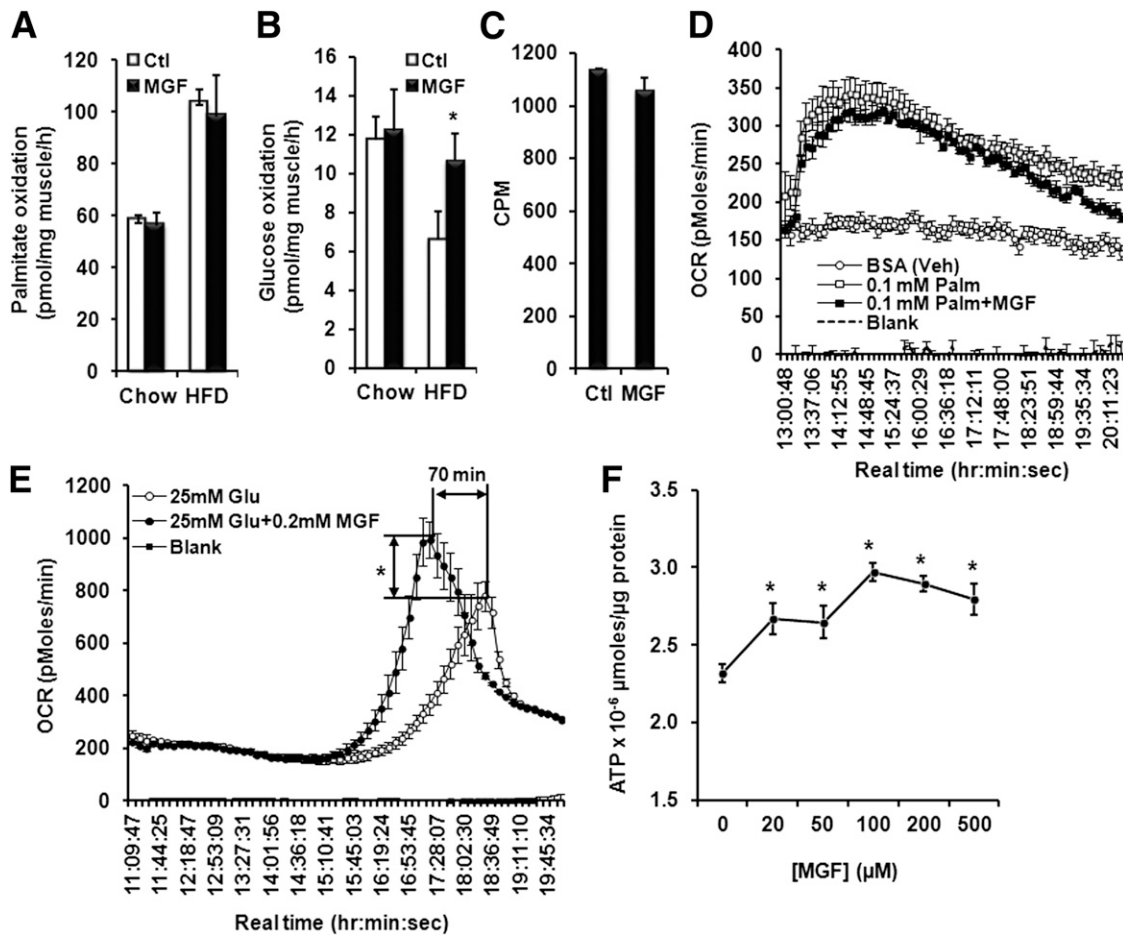


Figure 4—MGF stimulates glucose oxidation. Palmitate (A) and glucose (B) oxidation was measured after a 12-h fast in soleus muscle isolated from mice fed with CD or HFD, with or without 0.5% MGF, for 18 weeks ($n = 6-7$). C: [14 C]-labeled oleic acid oxidation in C2C12 myotubes pretreated or not with 200 $\mu\text{mol/L}$ MGF for 16 h. Palmitate (D) and glucose (E) oxidation in C2C12 myotubes measured by Seahorse Bioscience Metabolic Flux analyzer. Myotubes differentiated from C2C12 cells in XF24 microplates were incubated overnight in glucose-free and sodium pyruvate-free DMEM, with or without 200 $\mu\text{mol/L}$ MGF. OCR was recorded after injection of vehicle (D), BSA-conjugated palmitate (D), or D-glucose (E) into wells, with or without 200 $\mu\text{mol/L}$ MGF. F: Intracellular ATP levels in C2C12 myotubes incubated overnight in glucose-free and sodium pyruvate-free DMEM in the presence of various concentrations of MGF and then incubated in media containing 25 mmol/L glucose with matching concentrations of MGF for 8 h. ATP was determined using the CellTiter-Glo Luminescent Cell Viability Assay kit according to the manufacturer's instructions (Promega). In vitro experiments were conducted three to four times and each time with triplicates for each condition. Values are average \pm SEM. * $P < 0.05$. P values were obtained by t test.

but not fats (Fig. 4C and D), in myotubes. These data imply that metabolic mediators downstream of pyruvate could be pharmacodynamic targets of MGF. We therefore investigated a putative target, PDH, using two enzymatic activity assays. One is a spectrometry assay measuring the pyruvate-dependent production of NADH (28,29,37), and the other is a radioactivity assay directly measuring $^{14}\text{CO}_2$ production from [carboxy- ^{14}C]pyruvate oxidation. Using the spectrometry assay, we observed that MGF increased NADH production in a dose-dependent manner and was more effective than the known PDH activator DCA (30) (Fig. 6B). To confirm that the NADH increase was PDH-dependent, we added FP, a potent inhibitor of PDH. Upon addition of FP, MGF stimulation of NADH production was abolished, suggesting that MGF acts to increase NADH production via increases in PDH activity. From

the absorbance versus time plots, we analyzed initial velocities of NADH formation and determined that MGF dose-dependently increased the initial rates of PDH-catalyzed reactions (Fig. 6C). Treatments for 24 h caused greater increases than 15-min treatments, although the latter contributed a large portion of the former. The half-maximal effective concentrations (EC_{50}) of 24-h and 15-min MGF treatments were 184 ± 23 and 216 ± 35 $\mu\text{mol/L}$, respectively. This suggests that effects of MGF on PDH may be complex, having acute as well as inducible features.

To confirm these studies, we sought a more reliable assay that can directly measure PDH activity. Radio-labeled [carboxy- ^{14}C]pyruvate substrate was used to measure PDH activity. We determined that acute treatment with MGF for 15 min provides statistically significant

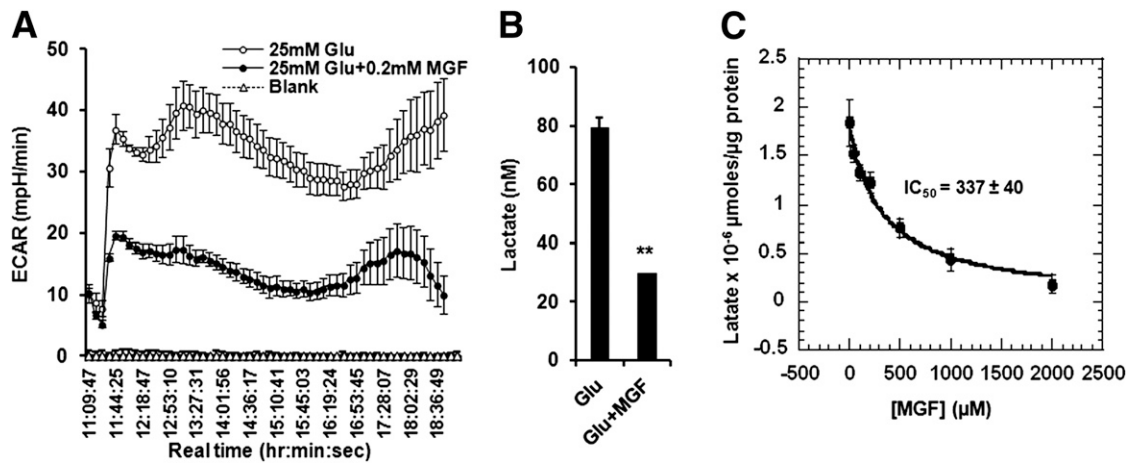


Figure 5—MGF inhibits lactic acidosis. *A*: ECAR recorded in the same Seahorse Bioscience Metabolic Flux experiments as shown in Fig. 4*E*. *B*: Lactate formed in the experiments shown in *A* was measured by a D-lactate assay kit. *C*: C2C12 myotubes were incubated overnight in glucose-free and sodium pyruvate-free DMEM containing L-glutamine and 2% horse serum, in the presence of various concentrations of MGF, and then incubated in media containing 25 mmol/L glucose in the presence of matching concentrations of MGF for 8 h. Media were collected, and lactate in the media was measured by a D-lactate assay kit (Eton Biosciences). These experiments were all conducted three to four times and each time with triplicates for each condition. Values are average \pm SEM. ** $P < 0.01$. P values were obtained by t test.

increases in PDH activity, with an EC_{50} of $234 \pm 37 \mu\text{mol/L}$ (Fig. 6*D*). The two sets of data obtained from two distinct methods (Fig. 6*C*, filled symbols; Fig. 6*D*) are in agreement, consistently showing that apparent PDH activity increased several fold and was ultimately saturated.

PDH is regulated by reversible phosphorylation by PDK(s) and PDH phosphatases (38). MGF treatment for 24 h resulted in a dose-dependent decrease in phosphorylated PDH (p-PDH) (Fig. 6*E* and *F*), consistent with increased PDH activity. Among four PDKs, PDK4 is highly expressed in muscle and sensitive to nutritional regulation and diabetic state (39,40). We assessed the effects of MGF on PDK4 and found that MGF dose-dependently suppressed PDK4 protein expression (Fig. 6*E* and *F*). In cells acutely treated with MGF for 15 min, MGF also reduced p-PDH (Fig. 6*G* and *H*), but did not change PDK4 expression level (data not shown), suggesting that acutely reduced p-PDH by MGF is probably due to inhibition of PDK activity. Inhibition of PDK(s) is the mechanism by which DCA activates PDH. MGF is more effective than DCA (Fig. 6*G* and *H*).

DISCUSSION

Excess dietary fat consumption and consequent excessive fatty acid utilization cause toxic impairments to glucose utilization, resulting in hyperglycemia, insulin resistance, and weight gain. In this respect, poor glucose utilization by the skeletal muscle has been identified as a major contributor to insulin resistance and weight gain associated type 2 diabetes (7). Strategies aimed to stimulate skeletal muscle bioenergetics as a direct approach to counteract diabetes have been pursued but have focused principally on mitochondrial activation and, particularly, increasing fatty acids oxidation. This strategy has been demonstrated to be of therapeutic interest and has

some impressive successes, but does have limitations because it does not specifically address poor carbohydrate utilization and possible corrective effects obtainable by increasing carbohydrate utilization as opposed to increasing fatty acid oxidation.

Here we report novel findings that address the fundamental question of whether it is feasible to correct metabolic syndrome by improving carbohydrate utilization selectively versus fatty acids. We discovered that MGF stimulates carbohydrate utilization even when fat is the predominant energy source. MGF was able to mitigate the negative consequences of excessive fat consumption and protect against diet-induced weight gain, hyperglycemia, glucose intolerance, hyperinsulinemia, and insulin resistance (Figs. 1 and 3*A–F*). In addition, it increases EE and preserves fuel utilization flexibility (Fig. 2*D, E, G, and H*). Increased RQ values with MGF treatment are consistent with stimulated carbohydrate utilization (Fig. 2*G*), which was confirmed in isolated muscle tissues and in cultured myotubes (Fig. 4).

Furthermore, we investigated the effects of MGF on the central metabolic switcher, PDH. The data from two assays consistently demonstrate that long- and short-term MGF treatments both potently increase PDH activity (Fig. 6*B–D*) and that this increase is, at least partially, due to reduced p-PDH resulting from MGF downregulation of PDK4 (Fig. 6*E–H*). HFD induces PDK4 (27,41), a mechanism by which HFD inhibits PDH activity, resulting in inhibition of carbohydrate utilization (41). MGF is able to suppress PDK4, and understandably, this effect could be more profound when PDK4 is induced by an HFD, which explains why the MGF-caused glucose oxidation increase under an HFD is greater than under a CD (Fig. 4*B*).

In line with the Randle cycle hypothesis (5,7), although MGF significantly enhanced carbohydrate oxidation, there

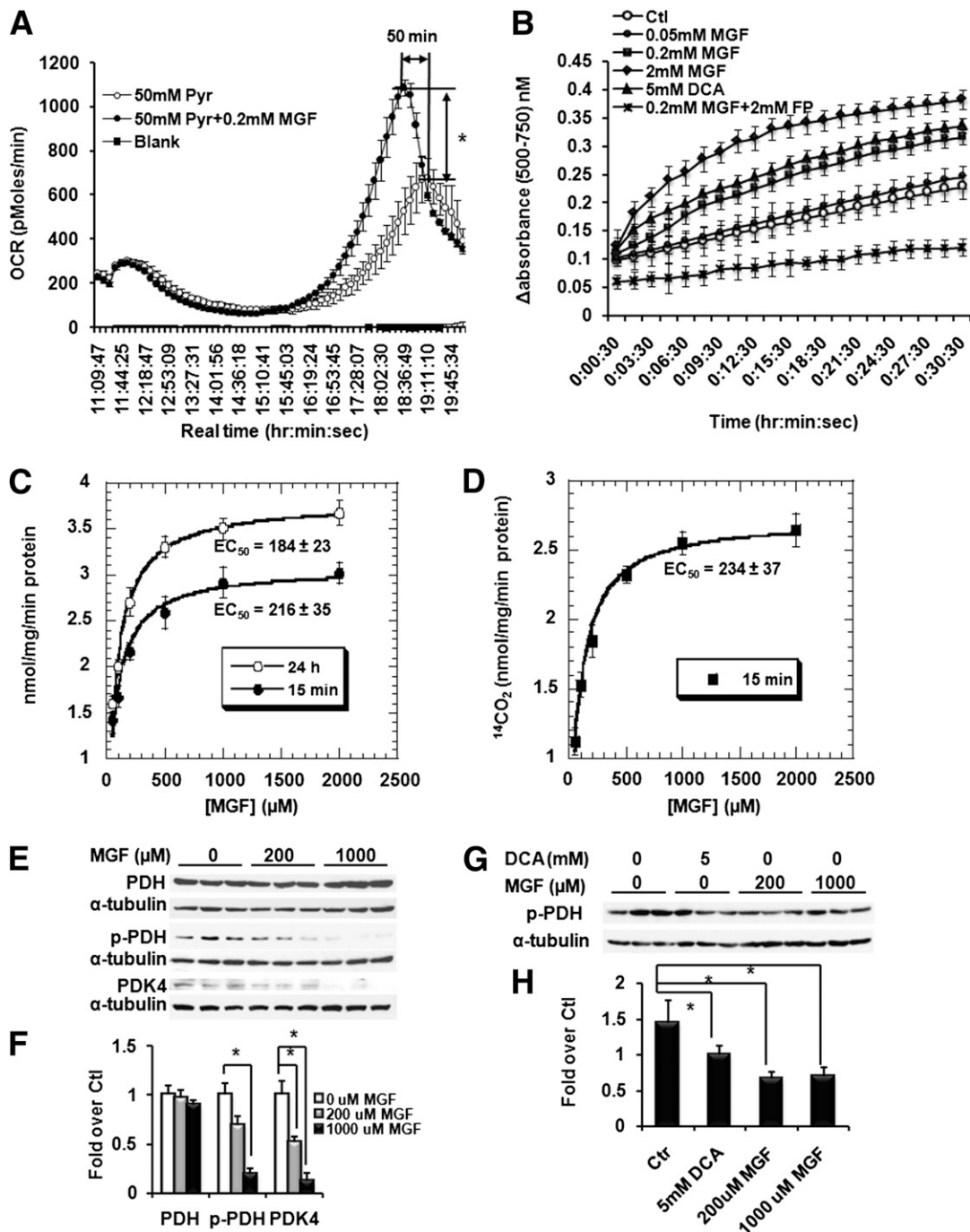


Figure 6—MGF enhances pyruvate oxidation by activating PDH. **A**: Pyruvate oxidation in myotubes differentiated from C2C12 cells measured by Seahorse Bioscience Metabolic Flux analysis. Myotubes differentiated from C2C12 cells in XF24 microplates were incubated overnight in glucose-free and sodium pyruvate-free DMEM, with and without 200 μmol/L MGF. OCR was recorded after injection of sodium pyruvate into wells, with or without 200 μmol/L MGF. **B**: PDH activities measured as the difference between absorbances at 500 nm and 750 nm at 25°C in mitochondrial protein from C2C12 myotubes treated with various concentrations of MGF for 24 h or 15 min or with 5 mmol/L DCA or FP + 200 μmol/L MGF for 15 min. **C**: Initial rates of PDH-catalyzed pyruvate oxidation measured as the difference between absorbances at 500 nm and 750 nm in mitochondrial protein from C2C12 myotubes treated with various concentrations of MGF for 24 h or 15 min. The unit of activity was determined by using extinction coefficient of reduced p-iodonitrotetrazolium violet (12.4 mmol · L⁻¹ · cm⁻¹). **D**: Initial rates of PDH catalyzed [¹⁴C]-labeled pyruvate oxidation measured as the production of ¹⁴CO₂ by mitochondrial protein from C2C12 myotubes treated with various concentrations of MGF for 15 min. **E**: Western blots of proteins extracted from C2C12 myotubes treated with 200 or 1,000 μmol/L MGF for 15 min and 24 h. Membrane was blotted with PDH (1:250 dilution; Cell Signaling), p-PDH (1:2,000; Abcam), PDK4 (1:500; laboratory of Dr. Robert Harris at Indiana University School of Medicine), or α-tubulin (1:2,000; Sigma-Aldrich) at 4°C overnight. **F**: Quantitative analysis of Western blots shown in **E**. **G**: Western blots of proteins extracted from C2C12 myotubes treated with 200 or 1,000 μmol/L MGF or 5 mmol/L DCA for 15 min. **H**: Quantitative analysis of Western blots shown in **G**. Values are average ± SEM. **P* < 0.05. *P* values were obtained by *t* test (**A**) or ANOVA test (**F** and **H**).

was a trend for reduced fatty acid oxidation in both muscle and C2C12 myotubes (Fig. 4A, C, and D). In hepatic tissues and cells, Niu et al. (42) observed that MGF increased oleic acid uptake and induced carnitine palmitoyl-transferase 1, suggesting that MGF possibly enhances fatty acid utilization in liver. These differences could reflect tissue-specific effects of MGF.

The PDH-catalyzed product acetyl-CoA can exit mitochondria to yield cytoplasmic acetyl-CoA, which serves as the substrate for de novo lipogenesis, suggesting that activation of PDH by MGF could potentially increase lipogenesis. Interestingly, our unbiased proteomics study revealed that MGF downregulated several critical enzymes in lipogenesis and predicted that MGF suppressed SREBP-1 (43), an important regulator of lipogenesis and adipogenesis (44,45). Further investigation uncovered that MGF inhibited adipogenesis in 3T3 L1 cells, probably by downregulating SREBP, as well as C/EBP and peroxisome proliferator-activated receptor- γ (data not shown). These inhibitory effects of MGF on lipogenesis and adipogenesis could be potential mechanisms by which MGF prevents HFD-induced obesity.

In addition, MGF enhanced adaptive thermogenesis (Fig. 2F), likely by activating brown adipose tissue uncoupling mechanisms (Supplementary Fig. 3). Besides inducing uncoupling proteins and presumably increasing energy leak/waste, MGF increases energy production as it increases ATP levels (Fig. 4F and Supplementary Fig. 5). We have shown that MGF induces enzymes catalyzing the tricarboxylic acid cycle and the electron transport chain (43). In addition, MGF raises the NAD⁺-to-NADH ratio (Supplementary Fig. 6), which propels the flux through the tricarboxylic acid cycle and the electron transport chain. These data suggest that MGF enhances mitochondrial bioenergetics, supporting the previous findings that MGF activates AMPK (42) and that activation of AMPK raises the NAD⁺-to-NADH ratio and increases mitochondrial bioenergetics (46).

Enhancing the mitochondrial respiratory chain could potentially increase reactive oxygen species. Interestingly MGF has well-established antioxidant properties because it bears a catechol moiety that enables it to form stable MGF-Fe²⁺/Fe³⁺ complexes, preventing Fenton-type reaction and lipid peroxidation (47). This antioxidant property could facilitate and maintain MGF activation of PDH, because PDH is susceptible to inactivation by reactive oxygen species (48). In turn, activation of PDH prevents O₂⁻ accumulation because PDH deficiency is associated with impaired mitochondrial O₂⁻ removal (49).

In summary, we report a novel small molecule, MGF, that is able to stimulate carbohydrate oxidation when fatty acid is the dominant energy source by enhancing the activity of PDH, a critical metabolic switcher, in the regulation of overall energy balance and homeostasis. Owing to its chemical structural features, oral MGF is bioavailable in rodent and human (25,50). Although the bioavailability of oral MGF is low, demanding a high

effective dose in vivo, and the EC₅₀ of MGF is in the micromole/liter range, those features make it possible for structural modification and activity enhancement. With the beneficial biological effects shown in this report, MGF represents a novel pharmacophore that has the potential to be developed into a therapeutic improving metabolic syndrome.

Acknowledgments. The authors thank Dr. Robert A. Harris, Indiana University School of Medicine, for generously providing the PDK4 antibody.

Funding. This work was supported by the grants that Y.C. received from the American Heart Association (0735066N), from the American Diabetes Association (1-11-JF-06), and partially from the National Institutes of Health/National Institute of Diabetes and Digestive and Kidney Diseases (DK-41296).

Duality of Interest. No potential conflicts of interest relevant to this article were reported.

Author Contributions. P.A. and C.C.B. researched data, contributed to discussion, and edited the manuscript. Z.L., K.S., O.B., D.Y.Y., X.L., W.L., and R.H.M. researched data. L.A.J. researched data and edited the manuscript. J.E.P. and R.H.M. contributed to discussion and edited the manuscript. A.A.S. contributed to experimental design and discussion and edited the manuscript. Y.C. proposed and designed the study, researched data, contributed to discussion, and wrote the manuscript. Y.C. is the guarantor of this work, and, as such, had full access to all the data in the study and takes responsibility for the integrity of the data and the accuracy of the data analysis.

Prior Presentation. Parts of this study were presented in poster form at the 72nd Scientific Sessions of the American Diabetes Association, Philadelphia, PA, 8–12 June 2012.

References

1. Danaei G, Finucane MM, Lu Y, et al.; Global Burden of Metabolic Risk Factors of Chronic Diseases Collaborating Group (Blood Glucose). National, regional, and global trends in fasting plasma glucose and diabetes prevalence since 1980: systematic analysis of health examination surveys and epidemiological studies with 370 country-years and 2.7 million participants. *Lancet* 2011; 378:31–40
2. Smyth S, Heron A. Diabetes and obesity: the twin epidemics. *Nat Med* 2006;12:75–80
3. Cantó C, Houtkooper RH, Pirinen E, et al. The NAD(+) precursor nicotinamide riboside enhances oxidative metabolism and protects against high-fat diet-induced obesity. *Cell Metab* 2012;15:838–847
4. Lagouge M, Argmann C, Gerhart-Hines Z, et al. Resveratrol improves mitochondrial function and protects against metabolic disease by activating SIRT1 and PGC-1 α . *Cell* 2006;127:1109–1122
5. Randle PJ, Garland PB, Hales CN, Newsholme EA. The glucose fatty-acid cycle. Its role in insulin sensitivity and the metabolic disturbances of diabetes mellitus. *Lancet* 1963;1:785–789
6. Nuutila P, Koivisto VA, Knuuti J, et al. Glucose-free fatty acid cycle operates in human heart and skeletal muscle in vivo. *J Clin Invest* 1992;89:1767–1774
7. Hue L, Taegtmeyer H. The Randle cycle revisited: a new head for an old hat. *Am J Physiol Endocrinol Metab* 2009;297:E578–E591
8. Hancock CR, Han DH, Chen M, et al. High-fat diets cause insulin resistance despite an increase in muscle mitochondria. *Proc Natl Acad Sci U S A* 2008;105:7815–7820
9. Turner N, Bruce CR, Beale SM, et al. Excess lipid availability increases mitochondrial fatty acid oxidative capacity in muscle: evidence against a role for reduced fatty acid oxidation in lipid-induced insulin resistance in rodents. *Diabetes* 2007;56:2085–2092
10. Kelley DE, Reilly JP, Veneman T, Mandarino LJ. Effects of insulin on skeletal muscle glucose storage, oxidation, and glycolysis in humans. *Am J Physiol* 1990; 258:E923–E929

11. Randle PJ, Priestman DA, Mistry S, Halsall A. Mechanisms modifying glucose oxidation in diabetes mellitus. *Diabetologia* 1994;37(Suppl. 2):S155–S161
12. Hall JL, Stanley WC, Lopaschuk GD, et al. Impaired pyruvate oxidation but normal glucose uptake in diabetic pig heart during dobutamine-induced work. *Am J Physiol* 1996;271:H2320–H2329
13. Olesen J, Killewich K, Pilegaard H. PGC-1 α -mediated adaptations in skeletal muscle. *Pflugers Arch* 2010;460:153–162
14. Zhou L, Cabrera ME, Okere IC, Sharma N, Stanley WC. Regulation of myocardial substrate metabolism during increased energy expenditure: insights from computational studies. *Am J Physiol Heart Circ Physiol* 2006;291:H1036–H1046
15. Stacpoole PW, Moore GW, Kornhauser DM. Metabolic effects of dichloroacetate in patients with diabetes mellitus and hyperlipoproteinemia. *N Engl J Med* 1978;298:526–530
16. Jeoung NH, Harris RA. Pyruvate dehydrogenase kinase-4 deficiency lowers blood glucose and improves glucose tolerance in diet-induced obese mice. *Am J Physiol Endocrinol Metab* 2008;295:E46–E54
17. Stein DT, Babcock EE, Malloy CR, McGarry JD. Use of proton spectroscopy for detection of homozygous fatty ZDF-drt rats before weaning. *Int J Obes Relat Metab Disord* 1995;19:804–810
18. Blouet C, Liu SM, Jo YH, Chua S, Schwartz GJ. TXNIP in Agrp neurons regulates adiposity, energy expenditure, and central leptin sensitivity. *J Neurosci* 2012;32:9870–9877
19. Muzumdar RH, Huffman DM, Atzmon G, et al. Humanin: a novel central regulator of peripheral insulin action. *PLoS ONE* 2009;4:e6334
20. Shortreed KE, Krause MP, Huang JH, et al. Muscle-specific adaptations, impaired oxidative capacity and maintenance of contractile function characterize diet-induced obese mouse skeletal muscle. *PLoS ONE* 2009;4:e7293
21. Yamada E, Pessin JE, Kurland IJ, Schwartz GJ, Bastie CC. Fyn-dependent regulation of energy expenditure and body weight is mediated by tyrosine phosphorylation of LKB1. *Cell Metab* 2010;11:113–124
22. García-Martínez C, Marotta M, Moore-Carrasco R, et al. Impact on fatty acid metabolism and differential localization of FATP1 and FAT/CD36 proteins delivered in cultured human muscle cells. *Am J Physiol Cell Physiol* 2005;288:C1264–C1272
23. Abe Y, Sakairi T, Kajiyama H, Shrivastav S, Beeson C, Kopp JB. Bioenergetic characterization of mouse podocytes. *Am J Physiol Cell Physiol* 2010;299:C464–C476
24. Nicholls DG, Darley-Usmar VM, Wu M, Jensen PB, Rogers GW, Ferrick DA. Bioenergetic profile experiment using C2C12 myoblast cells. *J Vis Exp* 2010;(46):2511
25. Han D, Chen C, Zhang C, Zhang Y, Tang X. Determination of mangiferin in rat plasma by liquid-liquid extraction with UPLC-MS/MS. *J Pharm Biomed Anal* 2010;51:260–263
26. Jeoung NH, Sanghani PC, Zhai L, Harris RA. Assay of the pyruvate dehydrogenase complex by coupling with recombinant chicken liver arylamine N-acetyltransferase. *Anal Biochem* 2006;356:44–50
27. Constantin-Teodosiu D, Cederblad G, Hultman E. A sensitive radioisotopic assay of pyruvate dehydrogenase complex in human muscle tissue. *Anal Biochem* 1991;198:347–351
28. Hinman LM, Blass JP. An NADH-linked spectrophotometric assay for pyruvate dehydrogenase complex in crude tissue homogenates. *J Biol Chem* 1981;256:6583–6586
29. Schwab MA, Kölker S, van den Heuvel LP, et al. Optimized spectrophotometric assay for the completely activated pyruvate dehydrogenase complex in fibroblasts. *Clin Chem* 2005;51:151–160
30. Sheu KF, Hu CW, Utter MF. Pyruvate dehydrogenase complex activity in normal and deficient fibroblasts. *J Clin Invest* 1981;67:1463–1471
31. Buffington CK, Kitabchi AE. Activation of pyruvate dehydrogenase complex (PDC) of rat heart mitochondria by glyburide. *Biochem Biophys Res Commun* 1984;123:202–209
32. Cate RL, Roche TE, Davis LC. Rapid intersite transfer of acetyl groups and movement of pyruvate dehydrogenase component in the kidney pyruvate dehydrogenase complex. *J Biol Chem* 1980;255:7556–7562
33. Miura T, Ichiki H, Hashimoto I, et al. Antidiabetic activity of a xanthone compound, mangiferin. *Phytomedicine* 2001;8:85–87
34. Heymsfield SB, Gonzalez MC, Shen W, Redman L, Thomas D. Weight loss composition is one-fourth fat-free mass: a critical review and critique of this widely cited rule. *Obes Rev* 2014;15:310–321
35. Garland T Jr, Schutz H, Chappell MA, et al. The biological control of voluntary exercise, spontaneous physical activity and daily energy expenditure in relation to obesity: human and rodent perspectives. *J Exp Biol* 2011;214:206–229
36. Trajcevski KE, O'Neill HM, Wang DC, et al. Enhanced lipid oxidation and maintenance of muscle insulin sensitivity despite glucose intolerance in a diet-induced obesity mouse model. *PLoS ONE* 2013;8:e71747
37. Birkenstock T, Liebecke M, Winstel V, et al. Exometabolome analysis identifies pyruvate dehydrogenase as a target for the antibiotic triphenylbismuthdichloride in multiresistant bacterial pathogens. *J Biol Chem* 2012;287:2887–2895
38. Roche TE, Baker JC, Yan X, et al. Distinct regulatory properties of pyruvate dehydrogenase kinase and phosphatase isoforms. *Prog Nucleic Acid Res Mol Biol* 2001;70:33–75
39. Sugden MC, Holness MJ. Mechanisms underlying regulation of the expression and activities of the mammalian pyruvate dehydrogenase kinases. *Arch Physiol Biochem* 2006;112:139–149
40. Constantin-Teodosiu D, Constantin D, Stephens F, Laithwaite D, Greenhaff PL. The role of FOXO and PPAR transcription factors in diet-mediated inhibition of PDC activation and carbohydrate oxidation during exercise in humans and the role of pharmacological activation of PDC in overriding these changes. *Diabetes* 2012;61:1017–1024
41. Crewe C, Kinter M, Szweda LI. Rapid inhibition of pyruvate dehydrogenase: an initiating event in high dietary fat-induced loss of metabolic flexibility in the heart. *PLoS ONE* 2013;8:e77280
42. Niu Y, Li S, Na L, et al. Mangiferin decreases plasma free fatty acids through promoting its catabolism in liver by activation of AMPK. *PLoS ONE* 2012;7:e30782
43. Lim J, Liu Z, Apontes P, et al. Dual mode action of mangiferin in mouse liver under high fat diet. *PLoS ONE* 2014;9:e90137
44. Eberlé D, Hegarty B, Bossard P, Ferré P, Fufelle F. SREBP transcription factors: master regulators of lipid homeostasis. *Biochimie* 2004;86:839–848
45. Kim JB, Spiegelman BM. ADD1/SREBP1 promotes adipocyte differentiation and gene expression linked to fatty acid metabolism. *Genes Dev* 1996;10:1096–1107
46. Cantó C, Gerhart-Hines Z, Feige JN, et al. AMPK regulates energy expenditure by modulating NAD⁺ metabolism and SIRT1 activity. *Nature* 2009;458:1056–1060
47. Andreu GP, Delgado R, Velho JA, Curti C, Vercesi AE. Iron complexing activity of mangiferin, a naturally occurring glucosylxanthone, inhibits mitochondrial lipid peroxidation induced by Fe²⁺-citrate. *Eur J Pharmacol* 2005;513:47–55
48. Tabatabaie T, Potts JD, Floyd RA. Reactive oxygen species-mediated inactivation of pyruvate dehydrogenase. *Arch Biochem Biophys* 1996;336:290–296
49. Glushakova LG, Judge S, Cruz A, Pourang D, Mathews CE, Stacpoole PW. Increased superoxide accumulation in pyruvate dehydrogenase complex deficient fibroblasts. *Mol Genet Metab* 2011;104:255–260
50. Hou SY, Wang F, Li YM, et al. Pharmacokinetic study of mangiferin in human plasma after oral administration. *Food Chem* 2012;132:289–294